Combustion Instability Problems Analysis for High-Pressure Jet Engine Cores

Michel Cazalens*
SNECMA, 77780 Moissy Cramayel, France
Sébastien Roux† and Claude Sensiau‡
Centre Européen de Recherche et de Formation Avancée en Calcul Scientifique, 31057 Toulouse, France
and
Thierry Poinsot§
Institut de Mécanique des Fluides de Toulouse, 31400 Toulouse, France

DOI: 10.2514/1.30938

The design of a clean combustion technology based on lean combustion principles will have to face combustion instability. This oscillation is often discovered late in engine development when, unfortunately, only a few degrees of freedom still exist to solve the problem. Individual component test rigs are usually not useful in detecting combustion instability at an early stage because they do not have the same acoustic boundary conditions as the full engine. An example of this unsteady activity phenomenon observed during the operation of a high-pressure core is presented and analyzed. To support the investigation, two numerical tools have been extensively used. First, the experimental measurement of unsteady pressure and the results of a multidimensional acoustic code are used to confirm that the frequency variations of the observed modes within the operating domain of the high-pressure core are due to the excitation of the first and second azimuthal combustor modes. The impact of acoustic boundary conditions for the combustor exhaust is shown to control the appearance and mode transition of this unsteady activity. Second, the three-dimensional reacting and nonreacting large eddy simulations for the complete combustor and for the injection system cup alone suggest that the aerodynamic instability of the flow passing through the cup could be the noise source exciting the azimuthal acoustic modes of the chamber. Based on these results, the air system (cup) was redesigned to suppress this aerodynamic instability, and experimental combustion tests confirm that the new system is free of combustion instability.

I. Introduction

THE high-pressure core used for the development of gas turbines consists of the association between a combustor chamber, a high-pressure compressor, and a high-pressure turbine (Fig. 1). Such devices are very useful for engine manufacturers because they are demonstrators used for the full assessment of advanced technology, which is intended to be put into service later for new engines. It is a very important step within the research and technological development process because the components, which have been designed and tested separately, will work together for the first time. Some new problems involving components' coupling, noise, and instability may appear during high-pressure core tests even if, during each individual component test campaign, no significant unsteady activity was detected. Combustion instabilities due to the interaction between acoustic and unsteady combustion are characterized by strong oscillations of pressure, velocity, and reaction rate and have been commonly observed in multiple industrial devices [1] since the first observations were made more than a century ago [2]. Sometimes, as a consequence of acoustic disturbance, some hydrodynamic bifurcations are observed leading to the creation of large-scale structures within the flow, which are parts of the combustion instability process. Even if the acoustic activity does not induce some corresponding structural vibrations, the generated noise level is usually regarded as unacceptable.

Today, lean combustion systems are promising devices to meet the future NOx emission reduction requirements. Unfortunately, they are also more sensitive to combustion instability compared with classical combustors for at least two reasons. First, lean combustion structures are more easily extinguished by turbulent fluctuations than the stoichiometric ones. As they can be reignited later in the combustor, they have the potential to become acoustic sources. Because the technological objective is to burn in a lean mode, the total percentage of the combustor occupied by lean combustion zones is increasing and, therefore, the probability of getting a more intense coupling between combustion and acoustics also increases. Second, because more air is flowing through the injection system, the probability of exciting hydrodynamic instability entering into the process of combustion instability is also increasing. As large-scale structures issued from the air system associated with the injection system control the mixing between fuel and air, they could lead to unsteady combustion and interactions with the acoustic waves to produce self-excited combustion oscillation.

The development of clean combustion devices based on lean combustion will be successful only if engine manufacturers implement the relevant knowledge and numerical methodology to reliably identify, analyze, and understand all of the related combustion instabilities appearing at each development stage (component level, high-pressure core level, and engine level) to find solutions and fully integrate combustion instability issues into the combustor design process to minimize their impact over the whole engine operating domain.

Moreover, to reduce the time and cost for development, engine manufacturers will probably increasingly run high-pressure cores without any previous component tests. At that point, controlling the complete process (identification, analysis, understanding,

Received 11 March 2007; revision received 11 September 2007; accepted for publication 6 February 2008.

*Combustion Design Reviewer, 2 Rd Point René Ravaud, Villaroche Center.
†Research Scientist.
‡Research Scientist.
§Research Director. Associate Fellow AIAA.

and proposition of solution) would appear to be of primary importance.

This paper presents an investigation methodology that has been successful in interpreting the high-pressure core experiment results. This methodology combines experiments and numerical methods in which large eddy simulation (LES) and acoustic analysis are the main components. LES has become a standard tool in the study of the dynamics of turbulent flames for gas turbines [3–17] or for piston engines [18], whereas acoustic analysis is a standard numerical method for predicting acoustic modes in cavities that has been extended to reacting flow cases by multiple authors in the past [12,19–21]. These tools will be described here briefly because the paper concentrates on the results they provide rather than on their theoretical basis. Section II presents the configuration and the related observed unsteady phenomena, whereas Sec. III briefly describes the numerical tools used for the work. Section IV focuses on analysis. Once the acoustic modes controlling the observed oscillations have been identified, a detailed discussion about their appearance, transition, and hysteresis is given. Hypotheses regarding the nature of the acoustic source at the origin of the phenomenon are formulated and verified. A general conclusion is made in Sec. V.

II. Configuration and Observed Phenomenon

The high-pressure core configuration includes a high-pressure compressor, a combustor, and a high-pressure turbine (Fig. 1). After a small delay past the ignition of the combustor, all of the unsteady pressure sensors (Fig. 1) mounted on the core engine indicate strong fluctuations (Fig. 2). For atmospheric operating core conditions, the oscillations appear at rotation speeds of around 9000 rpm. Because there is no mechanical response detected anywhere, this unsteady activity involves only aeroacoustic issues. By increasing the engine power, the unsteady activity disappears for rotation speeds of around 16,500 rpm. Usually sensors are installed at different axial and azimuthal locations on the core engine. For the present case, sensors C1–C6 are mounted at different azimuthal locations on the last stator stage of the high-pressure compressor. Others sensors are located on the combustor false igniter and in some cavities outside the main flow. For civilian applications, the combustor casing is designed to be equipped with two igniters. For high-pressure core testing, one igniter is sufficient and the other one is replaced by an unsteady pressure sensor, named the false igniter, which monitors the pressure inside the combustor.

Figure 3 displays the measured frequencies with respect to the combustor inlet temperature over several test days and reveals the following:

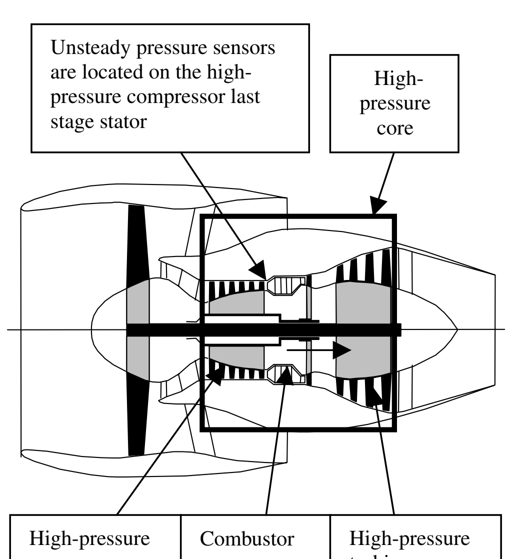

Fig. 1 Classical aeroengine structure.

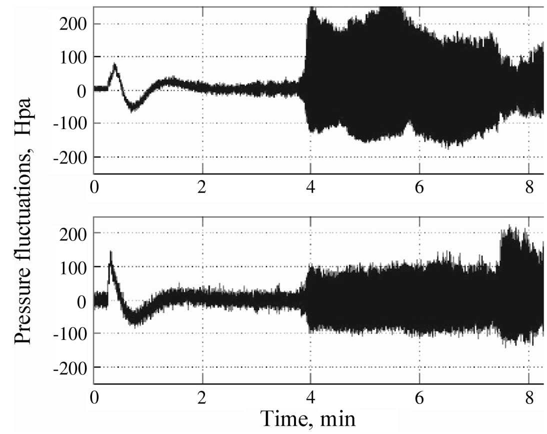

Fig. 2 Typical signals recorded by unsteady pressure sensors.

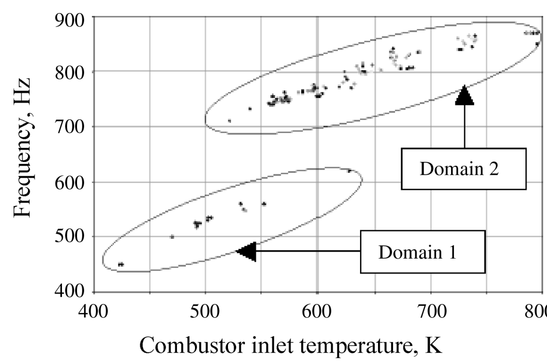

Fig. 3 Unsteady activity domains with respect to the combustor inlet temperature.

1) Unsteady activity frequencies are changing as the operating point of the core engine is changing, but they are not linear functions of the rotation speed.

2) Two different domains can be identified; within domain 1, frequencies are in the range of 400–600 Hz whereas within domain 2, they are in the range of 700–900 Hz.

3) The unsteady pressure signal amplitude is highly dispersed and does not exhibit any clear relation with the mechanical, aerodynamic, or thermodynamic operating parameters of the core engine.

For a given test day, the transition between domains 1 and 2 is abrupt and the frequency shift is around 300 Hz. The rotation speed of the core engine corresponding to transition during acceleration is not the same as the one corresponding to the transition from domains 2 to 1 during a deceleration. This hysteresis phenomenon suggests that the thermal behavior of the core engine could play a role in the process governing the transition between the two domains. This aspect will be specifically discussed later. Unsteady activity disappears roughly 0.2 s after the shutdown of the fuel flow. The rotation speed just begins to decrease and no dramatic aerodynamic change is expected at this time. This observation confirms that combustion is an essential ingredient for the existence of this instability process. It is not an aerodynamic noise amplified within some internal cavities because, in this case, it would continue to exist even when the fuel flow is stopped. Unsteady activity also disappears when the rotation speed exceeds 16,500 rpm, showing that certain regimes with combustion are also stable.

III. Numerical Tools

To study the unsteady behavior described in the previous section, four different solvers have been used:

1) AVBP. This LES solver [11] enables the solution of fully compressible Navier–Stokes equations in complex geometries. It has been validated successfully on numerous combustion chambers over the last five years [12–14,22–24]. LES has revolutionized the

capacities of computational fluid dynamics in the field of unsteady combustion by providing an insight into the large-scale structures present in the flow. Because combustion instability is most often associated with large-scale vortices, LES is the most obvious choice to study such phenomena.

2) N3S. This Reynolds-averaged Navier–Stokes (RANS) solver is used to compute the mean flow within the combustor using classical turbulence models.

3) NOZZLE. This is a one-dimensional acoustic solver that gives the impedances of nozzles such as the diffuser or the distributor located downstream from the combustion chamber

4) AVSP. This three-dimensional Helmholtz solver provides the solutions to the acoustic equations (frequencies and mode structure) in a domain in which the temperature and speed of sound are given by AVBP or N3S and impedances are estimated using NOZZLE. AVSP solves the wave equation in a nonisothermal three-dimensional domain [10,25]. This solver has been used in conjunction with AVBP and is useful in understanding experimental or LES results [21,26]. Although the LES of the complete combustor is feasible, a pure acoustic analysis is still valuable not only for cost and time delay reasons, but also to understand all of the possible oscillation modes; LES will only give the most amplified mode corresponding to a given set of boundary conditions, whereas the Helmholtz solver AVSP will provide all possible acoustic modes that can exist within the system in terms of frequency and the amplification factor.

IV. Analysis of the Instability Modes

A. Acoustics Analysis

Figure 4 displays pressure signals that are measured by sensors C1–C6 when the combustor operates in domains 1 and 2, respectively. A phase shift exists between all of the sensors, showing that the modes are not longitudinal. Sensors C1–C4 and C3–C6 are located on opposite sides just after the last high-pressure compressor stage and then just before the combustion chamber. For these two pairs of sensors, Fig. 4 shows that the phase difference between the pressure signals is close to π for domain 1 (compatible with uneven azimuthal modes) and zero for domain 2 (compatible with even azimuthal modes). To check whether the modes observed experimentally are linked to acoustics, AVSP was used for the complete combustor (Fig. 5a) and for several operating conditions of the core engine, covering the entire domain of interest. Five thermodynamics conditions have been chosen from the ones experienced by the core engine. For each condition, AVSP provides the frequency and the spatial structure of all of the acoustic modes that can exist within the system. The mesh used for AVSP is derived from the LES mesh performed on one sector; it includes the plenum

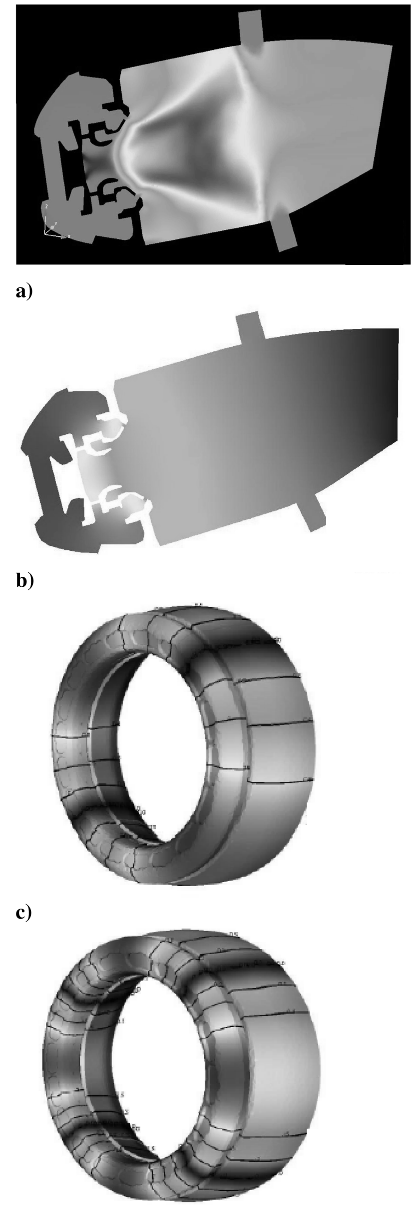

Fig. 5 Acoustics computations—inputs/outputs: a) configuration and speed of sound field, scale is from 340 to 995 m/s, b) structure of mode 1L, c) structure of the first azimuthal acoustic modes, and d) structure of the second azimuthal acoustic modes. Pressure fluctuation moduli are displayed for mode structure. Black colors indicate maximum pressure amplitude and white colors indicate pressure nodes.

Fig. 4 Typical signals recorded by the last high-pressure compressor stage unsteady pressure sensors when unsteady activity runs into domain 1 (left) and 2 (right).

and the injection system but does not include the turbine nozzle that is represented by its equivalent impedance calculated with NOZZLE. As the real chamber contains 18 injection systems, the global acoustical mesh is obtained by reproducing the mesh corresponding to one sector 18 times. The mean temperature fields needed by AVSP to compute the corresponding speed of sound fields are obtained from RANS computations with the N3S-NATUR code; the sound speed varies between 400 and 900 m/s. For each regime, as for the mesh itself, the speed of sound field is then reproduced 18 times in the azimuthal direction to obtain the complete speed of sound field for the combustor; a possible influence of the manufacturing variations of injection systems on the azimuthal temperature profile is not taken into account. The acoustic boundary conditions for AVSP correspond to the impedance computed by NOZZLE at the outlet and to velocity nodes for all inlets and walls. The results of acoustic computations are presented in Figs. 5 and 6. Figure 5b displays the structure of the first longitudinal mode (1L) in the symmetry plane of the chamber whereas Fig. 5c displays the structures of the first two

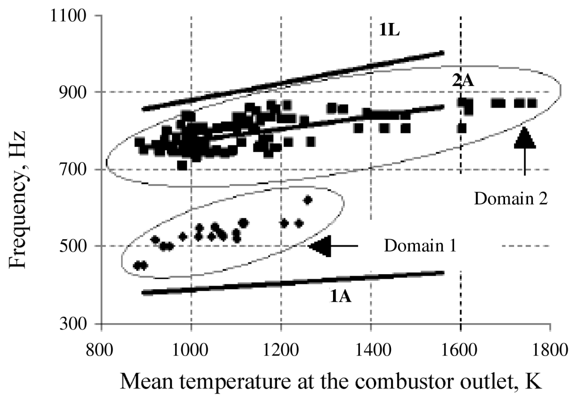

Fig. 6 Comparison of the evolution of unsteady activity frequency with the computed frequencies of the 1L, 1A, and 2A acoustical modes of the combustor.

azimuthal modes (1A and 2A). Figure 6 presents the frequency evolution for the first longitudinal mode (1L) and the first and second azimuthal ones (1A and 2A) as functions of the mean temperature at the combustor outlet. The same figure also displays the experimental recorded frequencies. Figure 6 indicates that the computed 2A frequency evolution over the domain of interest lies very well within the measured frequencies for domain 2 and exhibits the right slope. Moreover, the spatial structure of the computed 2A mode (Fig. 5c) is fully compatible with the one that can be perceived through the six pressure sensors C1–C6 (Fig. 4) suggesting that the second azimuthal mode of the plenum-combustor system (2A) is the mode appearing within domain 2. Note that this result shows that an oscillation mode (such as domain 2 in Fig. 3) with a frequency that changes with rotation speed can still be linked to an acoustic mode simply because acoustic frequencies also shift when the regimes change.

For the mode of domain 1, the analysis is more difficult because Fig. 6 indicates that the frequencies computed by AVSP are outside domain 1, whereas the azimuthal spatial structure that can be drawn from the recorded pressure signal is fully compatible with the one obtained for the computed first azimuthal mode. The mismatch in frequency (around 500 Hz experimentally for around 400 Hz in AVSP) is probably due to the fact that the boundary conditions are not perfectly identified in AVSP and are sufficiently small to conclude that the first azimuthal mode (1A) is observed within domain 1.

From the five computed thermodynamic conditions, we have derived a linear correlation giving the frequency of the 2A mode as a function of the average temperature at the combustor outlet. The 2A mode has been chosen because it is the one that is more often encountered during the operation of the high-pressure core and also because the fit of the computed acoustic frequency with the measured one is the best. A set of 200 operating conditions of the high-pressure core corresponding to several days of tests has been considered. Then the differences between the acoustic frequency obtained with the previous correlation and the measured ones were calculated for each operating condition. Thus, a table linking these differences to the amplitudes measured by the sensors at the last compressor stator stage and by the one inside the combustor is available (Table 1). To simplify the presentation, the 200 frequency differences have been distributed into five categories. For each category, the amplitude average is computed from the measured corresponding ones and the final results are synthesized into Table 1.

Table 1 clearly shows that the maximum amplitudes are obtained when the frequency of the instability corresponds, with a small dispersion, to the acoustic frequency of the combustor and demonstrates the thermoacoustic nature of the phenomenon. Moreover, the sensor located inside the combustor gives a stronger signal than the ones on the last compressor stator stage. Table 1 also shows that a background acoustic activity exists, which could be due to the activity of an unsteady source that should be identified.

B. Appearance, Transition, and Hysteresis

The previous section suggested that the mode responsible for the unsteady activity in domain 1 is the first azimuthal (1A), whereas the mode inducing oscillations in domain 2 is the second azimuthal (2A). The two acoustic modes can exist simultaneously or not depending on the thermodynamic state, the combustion distribution, and the acoustic boundary conditions. Indeed, during the operation of the core engine, at least two singularities can provide strong changes for the acoustic boundary conditions of the combustor. They correspond to regimes in which, first, the high-pressure turbine nozzle and, second, the first stage of the high-pressure turbine choke. As anticipated from Fig. 1, choking the turbine nozzle has an obvious impact on the acoustic boundary conditions at the outlet of the combustor. The choking of the first high-pressure row can have an impact on the acoustic boundary conditions of the combustor in two ways:

1) A coupling mechanism between the two shock waves can lead to a change in the acoustic boundary conditions or to a simple interaction/adaptation of the first shock to the presence of the second one. This mechanism alters the flow and acoustics near the combustor outlet.

2) All of the mass flow rate issued from the prediffuser does not enter the combustor and part of it flows into the combustor casing to cool the high-pressure turbine nozzle and the first row of vanes. Row choking can change acoustic impedances, and this information can be transmitted to the chamber through the external flow around the combustor thereby affecting all of the mass flow rates coming into the combustor, especially the one associated with the injection system. Although influence though primary holes, dilution holes, and effusion cooling is also possible, it is expected that the main effect is through the injection system.

If this scenario is true, a simple verification is that there should be coincidence, first, between the appearance of the unsteady activity and the turbine nozzle choking (around 8000–9000 rpm) and, second, between the transition and the choking of the high-pressure turbine first row (between 13,500 and 15,000 rpm). These tests have been performed experimentally over various test days and confirm this assumption by proving that unsteady activity on mode 1 begins when the turbine nozzle chokes and that mode 2 replaces mode 1 when the first high-pressure row of the turbine chokes. The thermal effects and dilatation affecting the geometric flow passage areas are different between the acceleration and deceleration of the core engine; therefore, as choking will not occur at the same rotation speeds for acceleration and deceleration, hysteresis is observed for the transition between the two acoustic modes.

C. Identification of the Source Exciting the Azimuthal Modes

The previous sections showed that the modes observed experimentally were two azimuthal modes of the chamber and that

Table 1 Average amplitude for each category

Category	Range of frequency difference, Hz	Average amplitude, mbar (last compressor stator stage)	Average amplitude, mbar (inside the combustor)
1	0–10	82	130
2	11–20	65	112
3	21–30	60	101
4	31–40	40	54
5	41–50	26	26

the choking of the passages downstream of the chamber was triggering these modes. This analysis is incomplete because the source of the oscillation is still unknown; acoustics alone cannot induce instability in the absence of a forcing mechanism. To identify this mechanism, additional LES and experiments were performed first for the combustor itself (with combustion, Sec. IV.C.1) and then for the injection system alone (without combustion, Sec. IV.C.2).

1. LES of the Combustor (Reacting Flow)

The previous experimental results can be analyzed in terms of Strouhal numbers; based on the air velocity at the injection system exit and on related characteristic dimensions, the Strouhal numbers of modes 1 and 2 vary between 0.2 and 0.5. This simple observation suggests that hydrodynamic modes might contribute to the unstable loop leading to modes 1 and 2; natural hydrodynamic instability in swirling sheared flow is known to produce large-scale turbulent structures that are able to provide the instability initiation mechanism through the induced oscillations of the mixing rate between air and fuel and of the reaction rate. To identify such large coherent structures, an analysis of the following operating point of the core engine ($T30 = 473$ K, $P30 = 4,4$ bar and $\mathrm{FAR} = 1,2\%$, where $T30$ and $P30$ represent the temperature and pressure, respectively, at the combustor inlet and FAR stands for the fuel–air ratio) corresponding to high levels of acoustic noise during the tests has been made using LES. Figure 7 displays the LES geometry that includes the high-pressure distributor at the chamber outlet to reproduce the corresponding acoustic condition (a complete analysis of the LES results is given in Roux's Ph.D. thesis [27]). At this regime, the high-pressure distributor is almost choked and its impedance is close to a choked nozzle (which means that it behaves acoustically almost like a rigid wall). The fuel is supposed to vaporize instantaneously when it enters the chamber and is injected on the burner axis (see Fig. 8).

Typical LES fields at random instants are given in Fig. 8. The flame is stabilized in the primary zone by the large swirl level. The isosurface of the stoichiometric mixture fraction allows a visualization of the natural instability mode observed in almost all swirling flows at these levels of swirl [28]; a precessing vortex core (PVC) exists on the chamber axis and moves both the rich zones and the flame front around the axis of the burner. This instability mode is not very strong in this case, in which the chamber is isolated from any upstream forcing, but it indicates a clear sensitivity in the frequency range of the PVC; the spectra of axial velocity obtained by LES on the burner axis (Fig. 9) reveals that the PVC appearing in this chamber is produced at a frequency ranging from 600 to 1200 Hz. The recirculation zone and the flame move in the same frequency range. This range contains the frequency of the mode observed in the experiment in domain 2 and corresponds to Strouhal numbers of the order of 0.6 that is typical of such flow. Even though this LES does not prove that the PVC is the source of the instability, it confirms that the chamber reacts strongly in this frequency range and that no upstream perturbation is needed to destabilize the flow inside the combustor. Therefore, the field of investigation can be reduced to the combustor module only.

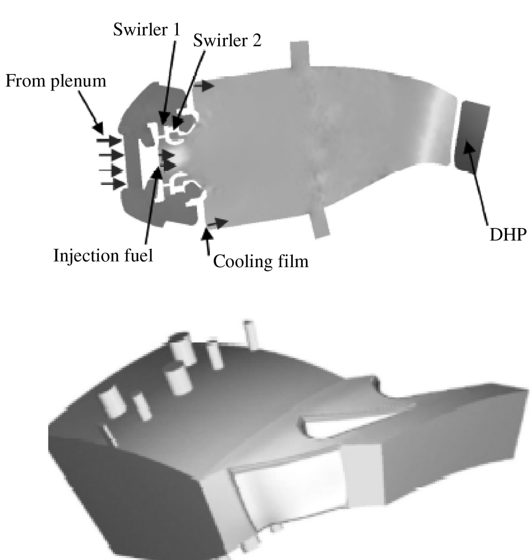

Fig. 7 Configuration for the LES computation (pressure field on a central cutting plane and global geometry), where DHP is the high-pressure turbine nozzle.

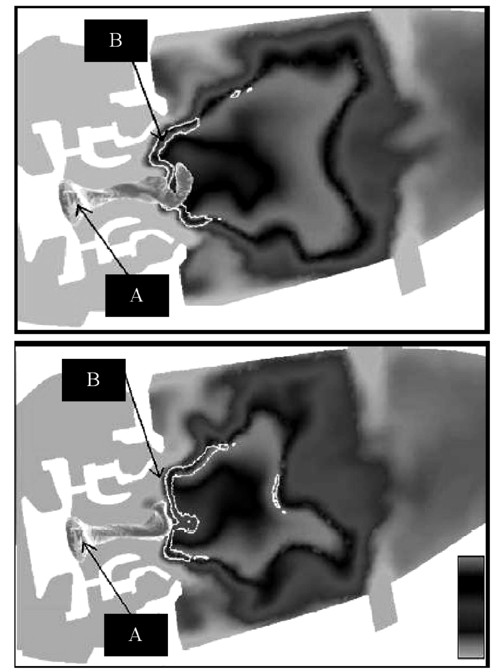

Fig. 8 Temperature field in the central cutting plane. B is the isosurface of the stoichiometric mixture fraction at two instants. A is the fuel injection. The temperature range is from 500 to 2600 K (dark regions).

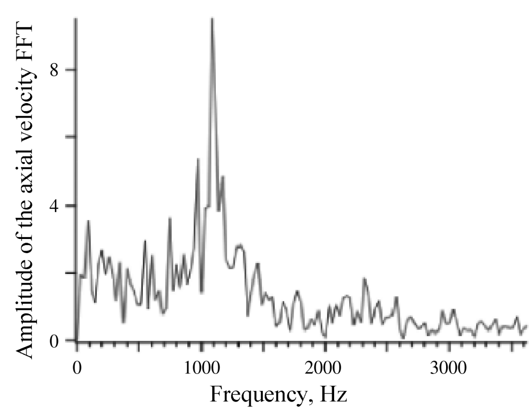

Fig. 9 Fast Fourier transform of the axial velocity at the exit of the injection system (computational data).

2. Experimental and LES Study of Injection System Unsteadiness (No Combustion)

The objective is now to confirm the previous findings for the complete range of operating conditions of the injection system and to identify technological modifications to suppress instability. Focus has been put on pure thermoacoustic behavior because no response of the fuel injector regarding possible unsteadiness of the liquid mass flow rate due to the acoustic wave has been detected during the operation of the high-pressure core in the presence of high-amplitude instability. The high liquid pressure loss at the injector tip, of more than 40 bar, implies that the acoustic wave has a very little impact on

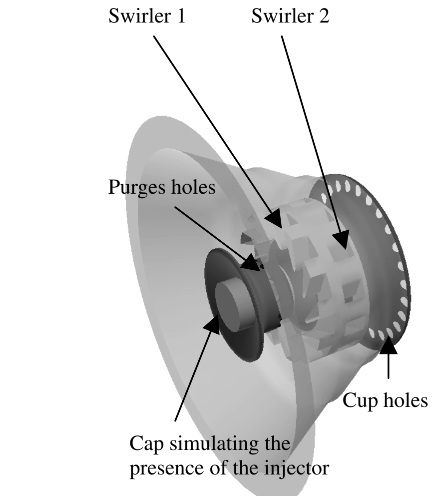

Fig. 10 Air system with a part of the experimental set up.

the fuel flow rate. Moreover, a mechanical analysis of the complete injector has shown that it cannot react for the frequency range involved in the analysis. Because it is not conceivable to modify the combustor geometry at this development step to make it insensitive to the perturbation induced by the source, changes to the air system associated with the injection system, to suppress the hydrodynamic source, have to be identified.

Figure 10 displays the air system associated with the injection system. It usually comprises five main elements: cup holes, purge holes, first swirler, second swirler, and a cooling system. The noise generated by the air system has been characterized from experimental results at an atmospheric pressure for different flow conditions. The air system was installed into a specific setup fed by air to generate different pressure drops from 1% to 6%. A microphone was installed some centimeters downstream from the

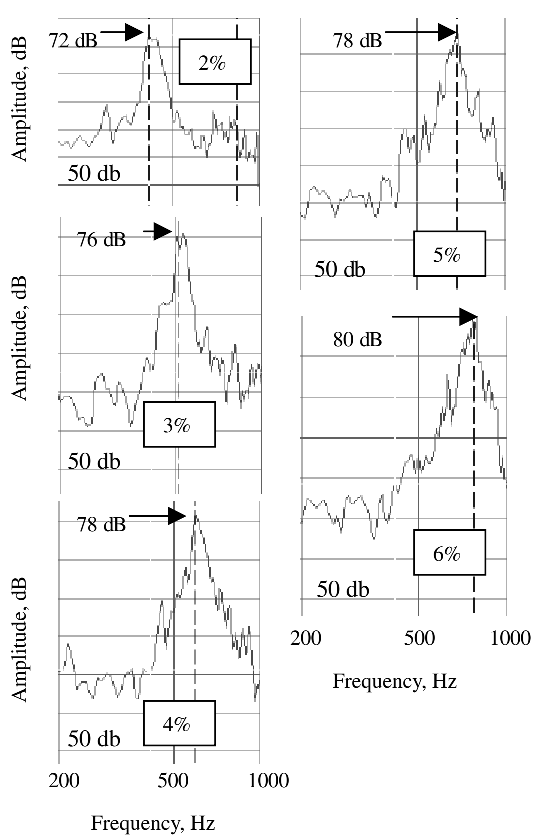

Fig. 11 Pressure spectrum for configuration 1.

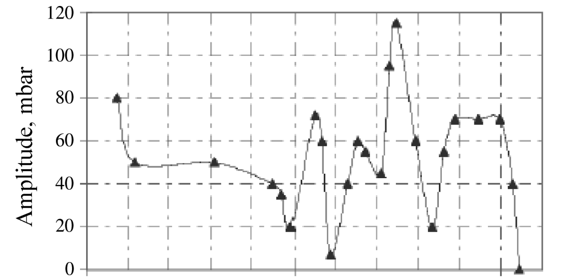

Fig. 12 One-hour temporal evolution of the unsteady activity amplitude.

setup. Postprocessing of the monitored values of unsteady pressure allows for the determination of the pressure spectrum for each operating condition (Fig. 11). For frequencies lower than 1000 Hz, a moving peak with respect to pressure drop is present. For a pressure drop equal to 1%, this peak is centered around 300 Hz; for a pressure drop equal to 4%, it is centered around 600 Hz; and for a pressure drop equal to 6%, it is centered around 800 Hz. This peak is intense and this result confirms the LES suggestion of the previous section, indicating that the air system could be the origin of the unsteady activity, acting as an acoustic source where frequency varies as a function of the flow velocity through the air system. The resulting unsteady activity amplitude depends on the amplification rate by combustion within the combustor. When the frequency peak coincides with the natural frequency of the combustor, the amplitude is expected to be high; otherwise, it remains low. This analysis seems to be confirmed by Fig. 12 displaying the evolution of the measured amplitude during an acceleration of the core engine and showing the large corresponding variations of amplitude and by the analysis given in Sec. IV.A.

To identify what elements or element combinations of the air system could be responsible for this hydrodynamic instability, some complementary tests have been made to obtain the acoustic spectra corresponding to the cases, described by Table 2, in which pressure loss varies from 1 to 6%.

Figures 13–17 display a zoom of the obtained acoustic spectra centered on the range of frequencies of interest for configurations 2–6 and for two pressure losses (2 and 6%). Because the scales are different between all the records, the maximum and the minimum amplitudes are directly indicated within the figures. Figure 13 suggests that this moving peak results from the hydrodynamic instability of the flow issued from the swirlers. Figures 14 and 15 indicate that only swirler 2 is involved in instability, with a possible amplification mechanism by a coupling with the flow of the purge holes (Fig. 16). Figure 17 demonstrates that the flow issued from the purge holes and from the cup holes does not generate any hydrodynamic instability. Because LES captures the dynamics of swirling flows rather easily [23], the complete experimental configuration has been computed for pressure losses equal to 4% and for the configurations that correspond to cases 1 and 3 in Table 2. The overall mesh is displayed in Fig. 18 and details of the mesh near the air system are provided in Fig. 19. A virtual sensor has been put into the computations to obtain the acoustic spectra to be compared with the experimental ones. Figure 20 indicates that the high amplitude acoustic peak is very well captured by LES at the right frequency whereas no particular acoustic activity can be detected in Fig. 21, as was expected from the previous experimental results. Therefore,

Table 2 Air system configurations

Case	Cup holes	Purge holes	Swirler 1	Swirler 2
1	Open	Open	Open	Open
2	Closed	Closed	Open	Open
3	Closed	Closed	Open	Closed
4	Closed	Closed	Closed	Open
5	Closed	Open	Closed	Open
6	Open	Open	Closed	Closed

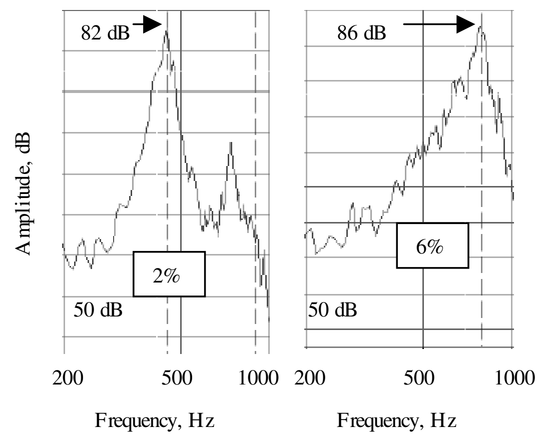

Fig. 13 Pressure spectrum for configuration 2.

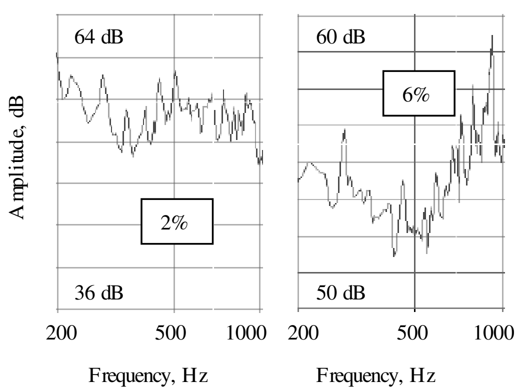

Fig. 14 Pressure spectrum for configuration 3.

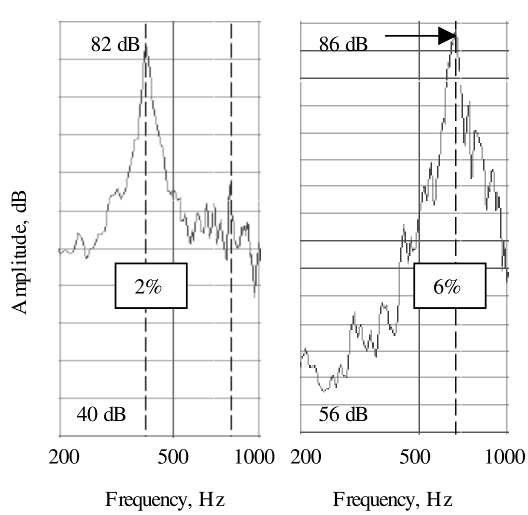

Fig. 15 Pressure spectrum for configuration 4.

LES will be considered as useful for the redesign process of the air system.

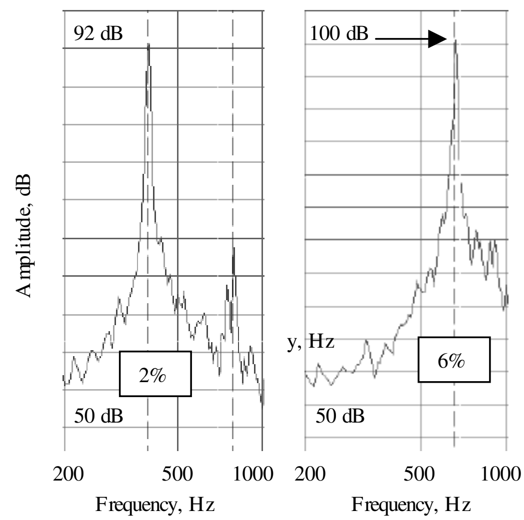

Fig. 16 Pressure spectrum for configuration 5.

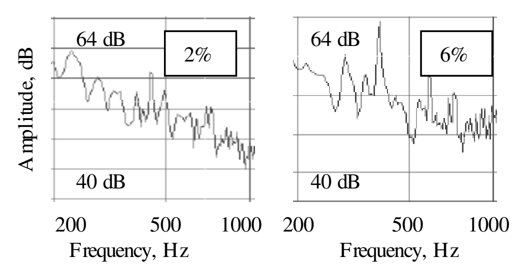

Fig. 17 Pressure spectrum for configuration 6.

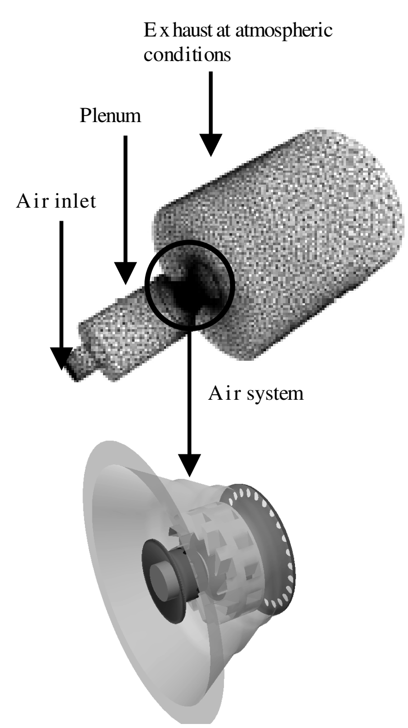

Fig. 18 Complete mesh for the nonreactive LES computations.

D. Modification of the Injection System to Solve the Problem

The previous analysis demonstrated that the air system was the origin of unsteady activity and needed a specific design optimization. Because of the need for NOx emission reduction, air system permeability has to be kept constant, and changes cannot be easily introduced because modifications brought to the air system can impact performance other than emission, such as temperature profiles at the exit of the combustor, a weak extinction limit, and the altitude restart domain. Changes have been applied to the airflow split of the air system (Table 3) and to the setting of the vanes of swirler 2 going from 60 to 45 deg to get an optimized design.

During the optimization process, LES computations of some other designs have been performed, and the selection of the optimized one has been made only from the analysis of the corresponding

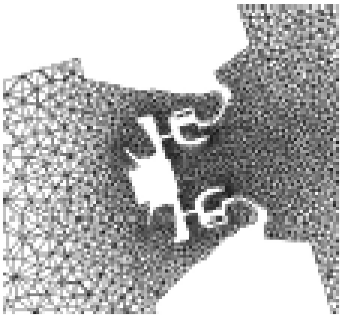

Fig. 19 Details of the mesh for the air system.

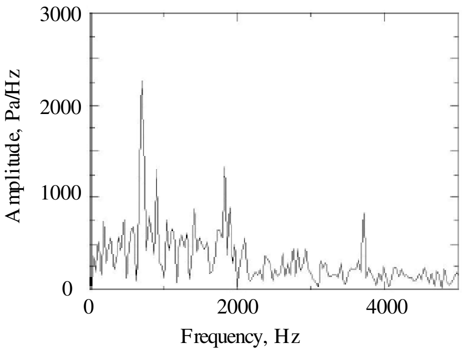

Fig. 20 Computed spectra for configuration 1.

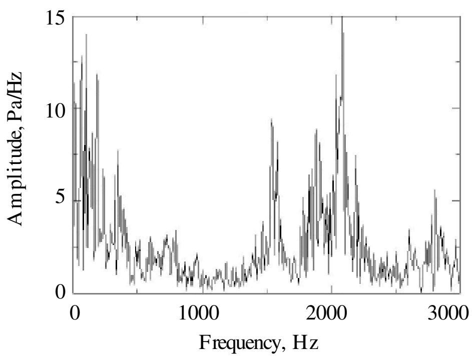

Fig. 21 Computed spectra for configuration 3.

computational results. The new system has been manufactured and tested without combustion in the setup of Sec. IV.C.2 with the same procedure as in Sec. IV.C.2. The corresponding acoustic spectrum for 4% pressure loss is displayed in Fig. 22. The comparison of Fig. 11 (corresponding to the initial design) with Fig. 22 (corresponding to the optimized design) reveals that the 600 Hz peak has disappeared. The same conclusion is obtained for the complete range of injection system operating conditions in terms of pressure loss. More important, the tests with combustion were repeated and, as expected, no unsteady activity was detected with the optimized air system.

Table 3 Details of the changes for the airflow split

Element	Current design	Optimized design
Purge holes	5%	2%
Cup holes	28%	32%
Swirler 1	24%	32%
Swirler 2	31%	24%
Cooling	11%	10%

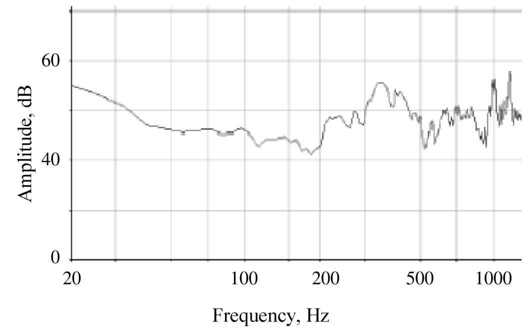

Fig. 22 Pressure spectrum for the modified injection system for a pressure drop of 4%.

V. Conclusions

The objective of the design of future lean combustion systems in gas turbine chambers is to make the combustor and injection systems free of any instability problem over their entire domain of operation. In the present research, experiments, LES, and acoustic modelling codes have been used together to analyze, understand, and solve a complex combustion instability problem occurring on a high-pressure core engine. This work demonstrates that the maturity level gained by numerical tools is now sufficient to complement experiments during the resolution of industrial problems at the design phase. This is a significant result because lean combustion is the strategy chosen by most engine manufacturers to make future engines more environmentally friendly in terms of pollution emissions. The present work also confirms the importance of acoustic boundary conditions both in the real world, because they control the oscillation modes, and in the numerical world, because they are needed to provide the correct predictions of unstable modes. This also suggests that the characterization of acoustic impedances at the high-pressure compressor outlet, at the combustor outlet for choked and nonchoked conditions, and for combustor walls when they are effusion cooled will be a major task in the future [29]. Because LES tools are at the core of the numerical process, it seems that further improvements regarding the capacity of LES to take into account two-phase flow and especially the influence of acoustics on the liquid phase from injection to evaporation will also be welcome.

References

[1] Lieuwen, T., and Yang, V., *Combustion Instabilities in Gas Turbine Engines: Operational Experience, Fundamental Mechanisms, and Modeling*, Vol. 210, Progress in Astronautics and Aeronautics Series, AIAA, Reston, VA, 2006.

[2] Rayleigh, L., "The Explanation of Certain Acoustic Phenomena," *Nature*, Vol. 18, July 1878, pp. 319–321.

[3] Janicka, J., and Sadiki, A., "Large Eddy Simulation for Turbulent Combustion Systems," *Proceedings of the Combustion Institute*, Vol. 30, No. 1, Jan. 2005, pp. 537–547. doi:10.1016/j.proci.2004.08.279

[4] Schildmacher, K., Hoffman, A., Selle, L., Koch, R., Schulz, C., Bauer, H-J., Poinsot, T., Krebs, W., and Prade, B., "Unsteady Flame and Flow Field Interaction of a Premixed Model Gas Turbine Burner," *Proceedings of the Combustion Institute*, Vol. 31, No. 2, Jan. 2007, pp. 3197–3205. doi:10.1016/j.proci.2006.07.081

[5] Boudier, G., Gicquel, L., Poinsot, T., Bissières, D., and Berat, C., "Comparison of LES, RANS and Experiments in an Aeronautical Gas Turbine Combustion Chamber," *Proceedings of the Combustion Institute*, Vol. 31, No. 2, Jan. 2007, pp. 3075–3082. doi:10.1016/j.proci.2006.07.067

[6] Sengissen, A., Giauque, A., Staffelbach, G., Porta, M., Krebs, W., Kaufmann, P., and Poinsot, T., "LES of Piloting Effects on Turbulent Swirling Flames," *Proceedings of the Combustion Institute*, Vol. 31, No. 2, Jan. 2007, pp. 1729–1736. doi:10.1016/j.proci.2006.07.010

[7] Sengissen, A., Poinsot, T., Van Kampen, J. F., and Kok, J. B., "Response of Swirled Non-Premixed Burner to Fuel Flow Rate Modulation," *Lecture Notes in Computational Science and Engineering*, Vol. 58, 2006, pp. 337–351.

[8] Giauque, A., Selle, L., Poinsot, T., Buechner, H., Laufmann, P., and Krebs, W., "System Identification of a Large Scale Swirled Partially Premixed Combustor Using LES and Measurements," *Journal of Turbulence*, Vol. 6, No. 21, 2005, pp. 1–20.
doi:10.1080/14685240512331391985

[9] Nicoud, F., and Poinsot, T., "Thermoacoustic Instabilities: Should the Rayleigh Criterion be Extended to Include Entropy Changes?," *Combustion and Flame*, Vol. 142, Nos. 1–2, July 2005, pp. 153–159.
doi:10.1016/j.combustflame.2005.02.013

[10] Poinsot, T., and Veynante, D., *Theoretical and Numerical Combustion*, 2nd ed., R. T. Edwards, Inc., Flourtown, PA, 2005, Chap. 8.

[11] Moureau, V., Lartigue, G., Sommerer, Y., Angelberger, C., Colin, O., and Poinsot, T., "High-Order Methods for DNS and LES of Compressible Multi-Component Reacting Flows on Fixed and Moving Grids," *Journal of Computational Physics*, Vol. 202, No. 2, Jan. 2005, pp. 710–736.
doi:10.1016/j.jcp.2004.08.003

[12] Selle, L., Lartigue, G., Poinsot, T., Koch, R., Schildmacher, K.-U., Krebs, W., Prade, B., Kaufmann, P., and Veynante, D., "Compressible Large-Eddy Simulation of Turbulent Combustion in Complex Geometry on Unstructured Meshes," *Combustion and Flame*, Vol. 137, No. 4, June 2004, pp. 489–505.
doi:10.1016/j.combustflame.2004.03.008

[13] Pitsch, H., "Large Eddy Simulation of Turbulent Combustion," *Annual Review of Fluid Mechanics*, Vol. 38, Jan. 2006, pp. 453–482.
doi:10.1146/annurev.fluid.38.050304.092133

[14] Schmitt, P., Schuermans, B., Geigle, K. P., and Poinsot, T., "Large-Eddy Simulation and Experimental Study of Heat Transfer, Nitric Oxide Emissions and Combustion Instability in a Swirled Turbulent High Pressure Burner," *Journal of Fluid Mechanics*, Vol. 570, Jan. 2007, pp. 17–46.
doi:10.1017/S0022112006003156

[15] Menon, S., and Patel, N., "Subgrid Modeling for Simulation of Spray Combustion in Large Scale Combustors," *AIAA Journal*, Vol. 44, No. 4, 2006, pp. 709–723.
doi:10.2514/1.14875

[16] James, S., Zhu, J., and Anand, M., "Large Eddy Simulation as a Design Tool for Gas Turbine Combustion Systems," *AIAA Journal*, Vol. 44, No. 4, 2006, pp. 674–686.
doi:10.2514/1.15390

[17] Huang, Y., Wang, S., and Yang, V., "Systematic Analysis of Lean-Premixed Swirl-Stabilized Combustion," *AIAA Journal*, Vol. 44, No. 4, 2006, pp. 724–740.
doi:10.2514/1.15382

[18] Thobois, L., Rymer, G., Soulères, T., Poinsot, T., and Van den Heuvel, B., "Large-Eddy Simulation for the Prediction of Aerodynamics in IC Engines," *International Journal of Vehicle Design*, Vol. 39, No. 4, 2005, pp. 368–382.
doi:10.1504/IJVD.2005.008468

[19] Stow, S., and Dowling, A., "Thermoacoustic Oscillations in an Annular Combustor," American Society of Mechanical Engineers Paper GT-0374, 2001.

[20] Walz, G., Krebs, W., Hoffmann, S., and Judith, H., "Detailed Analysis of the Acoustic Mode Shapes of an Annular Combustion Chamber," AIAA Paper 99-113, 1999.

[21] Martin, C., Benoit, L., Nicoud, F., and Poinsot, T., "Analysis of Acoustic Energy and Modes in a Turbulent Swirled Combustor," *AIAA Journal*, Vol. 44, No. 4, 2006, pp. 741–750.
doi:10.2514/1.14689

[22] Priere, C., Gicquel, L. Y. M., Gajan, P., Strzelecki, A., Poinsot, T., and Berat, C., "Experimental and Numerical Studies of Dilution Systems for Low Emission Combustors," *AIAA Journal*, Vol. 43, No. 8, 2005, pp. 1753–1766.
doi:10.2514/1.14681

[23] Roux, S., Lartigue, G., Poinsot, T., Meier, U., and Berat, C., "Studies of Mean and Unsteady Flow in Swirled Combustor Using Experiments, Acoustic Analysis and Large Eddy Simulations," *Combustion and Flame*, Vol. 141, Nos. 1–2, April 2005, pp. 40–54.
doi:10.1016/j.combustflame.2004.12.007

[24] Sommerer, Y., Galley, D., Poinsot, T., Ducruix, S., Lacas, F., and Veynante, D., "Large Eddy Simulation and Experimental Study of Flashback and Blow-Off in a Lean Partially Premixed Swirled Burner," *Journal of Turbulence*, Vol. 5, No. 1, March 2004, p. 37.

[25] Nicoud, F., Benoit, L., and Sensiau, C., "Acoustic Modes in Combustors with Complex Impedances and Multidimensional Active Flames," *AIAA Journal*, Vol. 45, No. 2, 2007, pp. 426–441.
doi:10.2514/1.24933

[26] Selle, L., Benoit, L., Poinsot, T., and Krebs, W., "Joint Use of Compressible LES and Helmholtz Solvers for Analysis of Rotating Modes in an Industrial Swirled Burner," *Combustion and Flame*, Vol. 145, Nos. 1–2, April 2006, pp. 194–205.
doi:10.1016/j.combustflame.2005.10.017

[27] Roux, S., "LES Methodologies for Gas Turbine Chambers," Ph.D. Thesis, Institut National Polytechnique de Toulouse, Toulouse, France, 2007.

[28] Syred, N., "A Review of Oscillation Mechanisms and the Role of the Precessing Vortex Core in Swirl Combustion Systems," *Progress in Energy and Combustion Sciences*, Vol. 32, No. 2, 2006, pp. 93–161.
doi:10.1016/j.pecs.2005.10.002

[29] Mendez, S., Nicoud, F., and Poinsot, T., "LES of a Turbulent Flow Around a Multi Perforated Plate," 2006 (To appear in Springer CY-LES).

T. Lieuwen
Associate Editor